Long-term drought intensification over Europe driven by the weakening trend of the Atlantic Meridional Overturning Circulation

M. Ionita [a,b,c,*], V. Nagavciuc [a,c], P. Scholz [a], M. Dima [a,d]

[a] Alfred Wegner Institute Helmholtz Center for Polar and Marine Research, Bremerhaven, Germany
[b] Emil Racovita Institute of Speleology, Romanian Academy, Cluj-Napoca, 400006, Romania
[c] Faculty of Forestry," Stefan cel Mare" University of Suceava, Suceava, Romania
[d] University of Bucharest, Faculty of Physics, Măgurele, Romania

ARTICLE INFO

ABSTRACT

Study region: Europe, with a particular focus on the Czech Republic, Poland, Spain, and Norway.
Study focus: Long-lasting droughts have become a semi-permanent feature of the European climate, especially over the last two decades. These prolonged droughts are usually driven by persistent sea surface temperature anomalies over the Pacific and Atlantic basins. By employing complex statistical methods (i.e., Canonical Correlation Analysis and Convergent Cross-Mapping) in this study we make a comprehensive assessment of the observed drying trend over the central and southern parts of Europe and its underlying drivers.
New hydrological insights: Building upon the potential relationship between drought variability and large-scale oceanic and atmospheric circulation, we show that the observed drying trend in the central and southern parts of Europe has been driven by a long-term slowdown of the Atlantic Meridional Overturning Circulation (AMOC), via changes in the large-scale atmospheric circulation. A weakening of AMOC leads to an increase in the frequency of atmospheric-blocking like circulation over the central part of Europe, which in turn inhibits precipitation and favors long-term drying. Since climate projections indicate a slowdown of the AMOC in the future, we suggest that this will potentially lead to an increase in the frequency of dry years, especially over the central and southern parts of Europe (e.g., the eastern part of Germany, the Czech Republic, Poland, Spain and Portugal).

1. Introduction

Since the early 2000s, Europe has become a 'hot spot' for high-intensity droughts, resulting in significant socio-economic losses (e. g., forest fires, agriculture and livestock farming like significant drop in EU cereal production, disruption of the inland waterway transport, stress on the public water supply and environmental degradation, among others) (Bakke et al., 2020; Ionita et al., 2021; Ionita and Nagavciuc, 2021; Spinoni et al., 2016; Stahl et al., 2016). Prolonged drought events pose a range of risks (e.g., lack of water for drinking water supply, irrigation, industrial use and power production, hindrance to navigation and deterioration of water quality, restriction/disruption of the industrial production process, sport/recreation facilities affected by a lack of water, tourism, fish fatalities

---

and stress on other aquatic fauna, reduced productivity of annual crop cultivation) to society, economy, environment, and biodiversity. How these long-lasting droughts are managed directly affects their costs and overall impacts. Depending on the type of drought (e.g., meteorological, hydrological, soil moisture, and/or societal), the overall impacts of lengthy and high-intensity droughts are felt across different sectors (e.g., agriculture, inland waterway transport, availability of drinking water, ecology, tourism). Over the past 5 years, more than a half of Europe has been affected by extreme drought conditions, with significant impacts on agriculture, inland waterway transport, forestry, society, and biodiversity (Bakke et al., 2020; Hari et al., 2020; Ionita et al., 2020; Ionita and Nagavciuc, 2020; Schuldt et al., 2020). In addition, climate projections indicate that Europe will become one of the hotspots for future high-intensity droughts and prolonged heatwaves, with southern and central Europe becoming increasingly dry and hot, and Fennoscandia becoming wetter and colder (Balting et al., 2021; Cook et al., 2020; IPCC, 2018; Naumann et al., 2018; Spinoni et al., 2019, 2018). For example, in terms of damages and impacts, the 2003 drought event affected large parts of central Europe, including the northwestern parts of Spain, France, Italy, Germany, Switzerland, and Austria, and the western part of the Czech Republic, leading to 17.134 billion Euro in direct impact (EEA, 2019). The 2015 drought event affected mostly the central and eastern parts of Europe and it was the hottest and climatologically driest summer over the 1950–2015 study period for an area stretching from the eastern Czech Republic to Ukraine (Ionita et al., 2017). The socio-economic impact in 2015 (~1250 deaths and 2.172 billion Euro of direct impact (EEA, 2019)) was much lower compared to the 2003 event, due to the awareness of the risk and vulnerability of the drought events. In a recent study (Naumann et al., 2021), has shown that over the period 1981 – 2010 droughts were responsible for around 9 billion € of damages per year to the economies of countries in the EU and the UK, and this value is expected to rise as economies grow and temperatures increase. Therefore, a better understanding of drought characteristics and their large-scale drivers at the European level is essential for better drought monitoring and forecasting in order to provide reliable adaptation strategies and thus reduce socioeconomic losses.

One of the most important drivers of long-lasting dry events over Europe is the North Atlantic sea surface temperatures (SST) (Ionita et al., 2012; Kingston et al., 2015; Schubert et al., 2014). For example, the 2015 drought event in the central part of Europe was mainly driven by anomalously cold SST anomalies in the North Atlantic basin (the so-called "cold blob", Duchez et al., 2016; Ionita et al., 2017). This cold blob, characterized by an anomalously negative SST anomaly south of Greenland, was associated with a $\sim 15\%$ weakening of the Atlantic Meridional Overturning Circulation (AMOC) since the middle of the 20th century (Dima and Lohmann, 2010; Rahmstorf et al., 2015), under influence of increasing atmospheric CO_2 concentrations (Dima et al., 2021). Since the AMOC plays a crucial role in transporting heat northward, a slowdown or a shutdown could lead to widespread cooling over the Northern Hemisphere, particularly around the east coast of U.S and the west coast of Europe (Jackson and Wood, 2020; Liu et al., 2020, 2017; Vellinga and Wood, 2008). To our knowledge, there is no study focused on a potential direct link between the observed AMOC changes and the drought features over Europe through the observational record. Therefore, building up on previous findings which indicate that, on monthly to interannual time-scales, persistent large-scale SST anomalies influence the frequency of drought events over Europe, in this study, we investigate the potential relationship between the long-term changes in drought over Europe and the weakening trend of the Atlantic Meridional Overturning Circulation.

2. Data and methods

The main variable analyzed in our study is the Standardized Precipitation Evapotranspiration Index (SPEI). SPEI was computed based on the monthly precipitation (PP), monthly mean air temperature (TT), and the potential evapotranspiration (PET) data from the CRU TS v. 4.04 dataset (Harris et al., 2020) using the R-package SPEI (https://cran.r-project.org/web/packages/SPEI/index.html). The SPEI computation is based on the probability distribution of the difference between PP and PET (PP– PET) and the data are normalized into a log-logistic probability distribution to obtain the SPEI (Vicente-Serrano et al., 2010). The potential evapotranspiration data were computed by employing the Penman–Monteith equation (Vanderlinden et al., 2008). Since the aim of our study is to analyze the observed trends in the long-term drought, at European level, we focus our analysis on an accumulation period of 12 months for SPEI (SPEI12). Thus, for the current study, we make use of December SPEI12, which integrates the drought variability throughout the whole year. To analyze the relationship between drought variability and the North Atlantic SST, we make use of the HadISST data set, with data distributed on a $1° \times 1°$ grid (Rayner et al., 2003) and covering the period 1871–2021. For the current study, we used the period 1901 – 2020, which overlaps with the time period when we have available data to compute SPEI.

In order to identify large-scale atmospheric circulation patterns associated with dry conditions over Europe, we use the monthly sea level pressure (SLP) fields from the 20th Century Reanalysis data V3, covering January 1902 to December 2015 period, with a spatial resolution of $2° \times 2°$ (Slivinski et al., 2021).

The trend analysis for the December SPEI12 field was performed by using the Mann-Kendall test (Mann, 1945). The Mann–Kendall test has been intensively used to identify trends in the hydrometeorological time series (Adamowski et al., 2009; Dang et al., 2020 and the references therein). The significance of a trend is determined by the Z statistic that has a normal distribution with a mean of 0 and a variance of 1. A positive Z value indicates an increasing trend, whereas a negative Z value shows a decreasing trend in the time series. The non-parametric Sen's slop method (Sen, 1968) was used to evaluate the magnitude of the trends.

The coupled modes of variability between SPEI12 and annual SST are obtained by applying the Canonical Correlation Analysis (CCA) technique. CCA is a powerful multivariate method used to identify pairs of patterns with the maximum correlation between their associated time-series (von Storch and Zwiers, 1999). In this study, we use the CCA to identify the main coupled modes of variability and their associated time components in the December SPEI12 and annual SST fields. Before applying CCA, the dimensionality of the SPEI12 and SST fields was reduced through an empirical orthogonal functions (EOF) analysis. The first 10 EOFs of SPEI12 and SST were retained as input in the CCA. For December SPEI12 the first 10 EOFs capture ~80 % of the total variance, while the first 10 EOFs of the annual SST capture ~85 % of the total variance.

In order to remove the uniform global warming trend, before applying the CCA between the SPEI12 and annual SST fields, we removed the yearly global average from each grid point. Dima et al. (2021) have demonstrated that this technique removes the spatially quasi-uniform nonlinear trend determined from data without the necessity to choose a linear or nonlinear shape to be removed a priori. In this respect, this method considerably improves the signal-to-noise ratio in the examined datasets since the globally consistent warming trend explains a large amount of variance in the initial SST field.

To investigate the potential causal relationships between annual SST (variable X) and December SPEI12 (variable Y), we used the Convergent Cross-Mapping (CCM) method, which relies on time embedded state space reconstruction based on data (Sugihara et al., 2012). An attractor is reconstructed based on each of the two-time series. If the variables are causally linked, then they are components of the same dynamical system. Consequently, their individual phase-space representations are projections of the common system's attractor and are topologically equivalent. Nearby points in the attractor of *Y* will correspond to nearby points in the attractor of *X*. If only *X* causes *Y*, then *Y* will contain information about *X*, but the time evolution of *X* is independent of *Y* and the former variable does not contain information about the later. CCM determines how well local neighborhoods on the attractor of X (a "library" of points) correspond to local neighborhoods on the phase space representation of Y. Thus, in the attractor of Y one finds nearest neighbors to a given point at time t and construct weights from them. Using these weights, an estimate of *X* at time t is generated based on its nearest neighbors in the X phase space representation. This procedure to compute X is repeated for all values of *Y* from the library of points. The similarity between the predicted and observed X time segments – the cross-map estimation – is quantified by the Pearson's correlation coefficient. The Pearson's correlation coefficient, which compares the observed and the predicted values, is used to measure prediction accuracy. In practice, the saturation of a cross-map between X and Y variables at a plateau above the significance thresholds suggests a causal relationship between the two variables (Dima et al., 2021; Sugihara et al., 2012). An increase in the library size corresponds to a better filled attractor and closer neighbors. Therefore, the correlation coefficient between predicted and observed X time segments should grow. This increase in the correlation is called convergence and distinguishes causation from correlation (Dima et al., 2021; Sugihara et al., 2012).

3. Results and discussion

The spatial pattern of the Mann–Kendall trend statistics (Mann, 1945) for the December SPEI12, for the period 1902–2020, is presented in Fig. 1. Negative values (brown) indicate a trend towards drier conditions, while positive values (green) indicate a trend towards wetter states. December SPEI12 exhibits a very clear signal: most of the countries in the southern and central parts of Europe show a significant decreasing trend (drying) over the last 120 years, while the countries in the northern part of Europe exhibit a significant positive trend (wetting). This is in agreement with the results from a recent study (Ionita and Nagavciuc, 2021), in which it
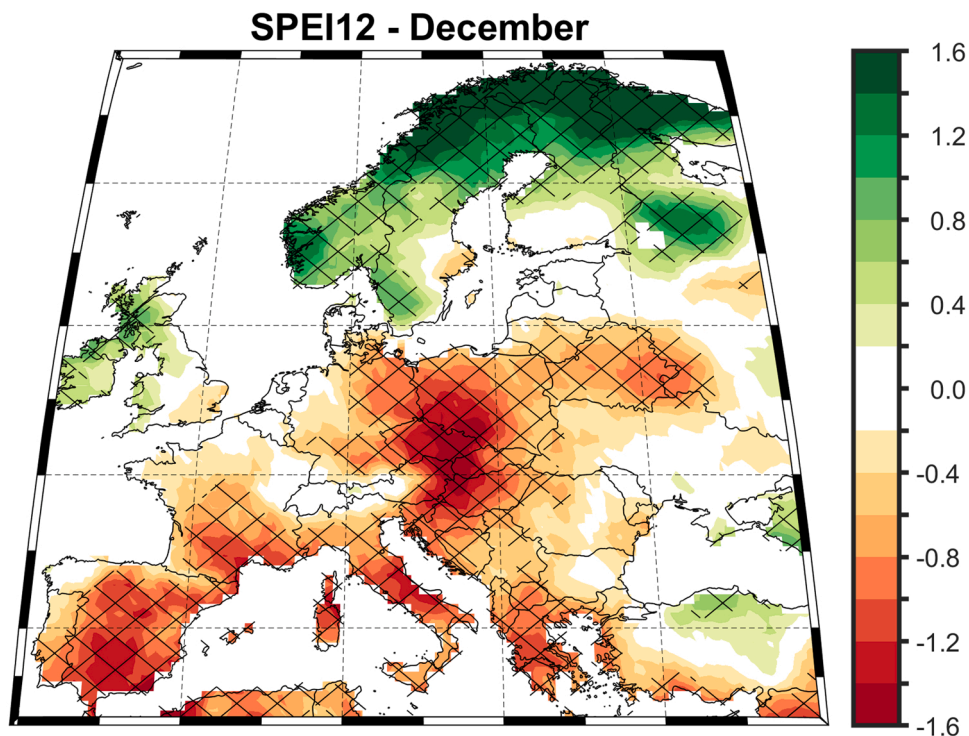

Fig. 1. Linear trend of the December Standardized Precipitation Evaporation Index for an accumulation period of 12 monthly (SPEI12). Stipples indicate statistically significant trends (95 % signficance level). Analyzed period: 1902–2020. Units: z scores/119 years.

has been shown that drought indices which take into account the effect of temperature (e.g. SPEI and the self-calibrated Palmer Drought Severity Index) show a drying trend over the southern and central parts of Europe and a wetting trend over the northern part of Europe, while precipitation-based drought indices (i.e. the Standardized Precipitation Index) do not capture this drying trend. The hotspots, in terms of drying, are Spain, Portugal, the southern part of France, Italy, the eastern part of Germany, the Czech Republic, Poland, Hungary, Slovenia, and Croatia. The hotspots in terms of wetting are northern part of U.K., Norway, Finland and Sweden (Fig. 1). This dipole-like structure between the central and southern parts of Europe and the north-western part of Europe is very clear also when looking at the probability distribution function of December SPEI12 averaged at country level (Fig. 2). The 30-years probability density function (PDF) for some of the countries affected by the drying trend over the last 120 years (i.e. the Czech Republic – Fig. 2a, Poland – Fig. 2b, Spain – Fig. 2c) shows a very clear pattern: the period 1991–2020 was the driest one over the observational record, while the period 1902–1930 was the wettest one. In the case of the countries which show a wetting trend (i.e. Norway – Fig. 2d) the pattern is rather opposite, the period 1991–2020 being the wettest one, while the period 1902 – 1930 being the driest one.
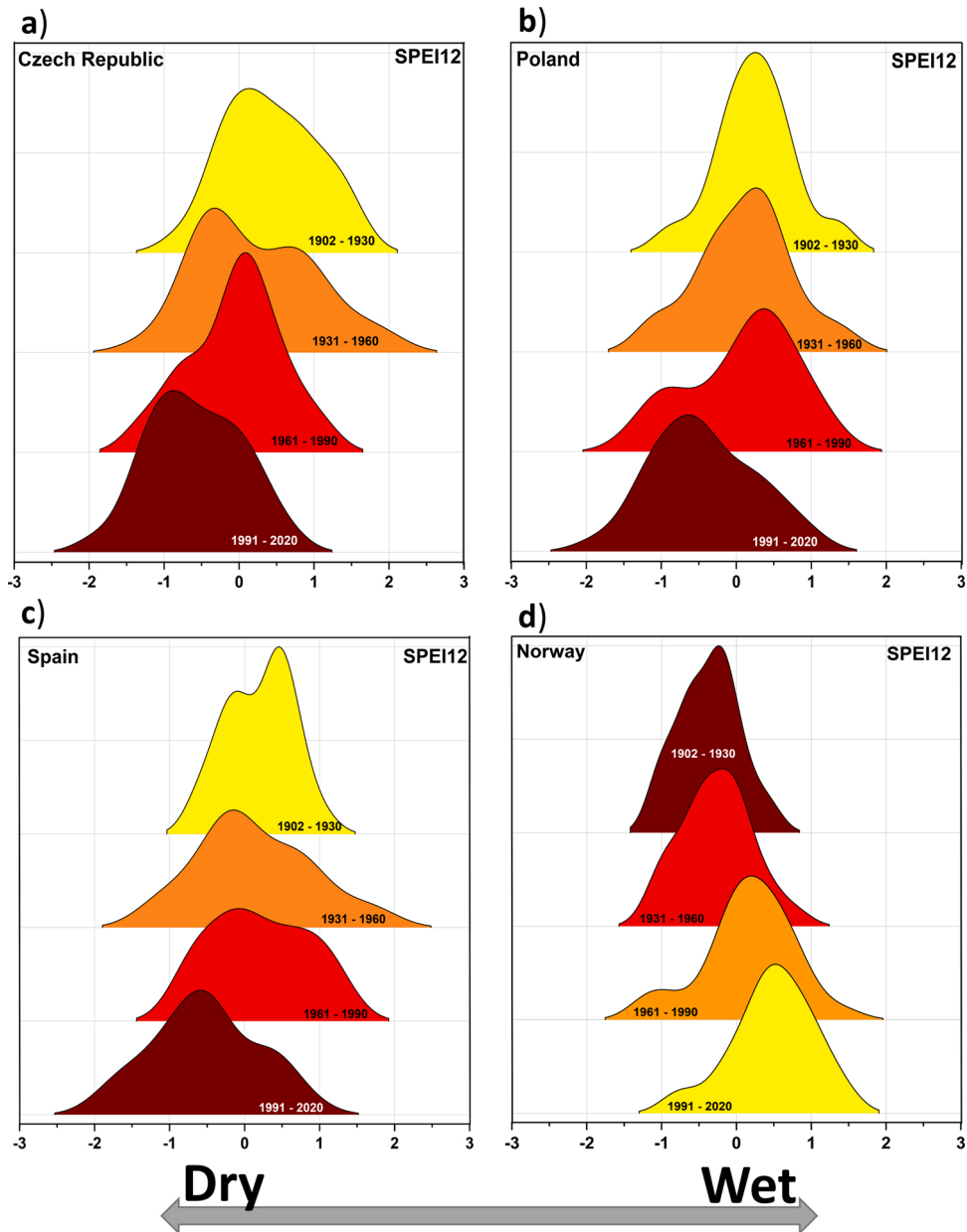

Fig. 2. The probability distribution function of December SPEI12 for different periods averaged at country level: a) the Czech Republic, b) Poland, c) Spain and d) Norway.

The temporal evolution of December SPEI12 averaged over some of the countries affected by the drying trend (i.e., Czech Republic – Fig. 3a, Poland – Fig. 3b, Spain – Fig. 3c) and the wetting trend (i.e., Norway) indicates strong interannual variability of the drought conditions, at country level, as well as a statistically significant drying (wetting) trend of the long-term drought condition (i.e., SPEI12). For the Czech Republic, Poland, and Spain, the occurrence of wet years was much higher before 1980′s compared to the period 1981 – 2020. After the beginning of the 1980′s, there are just a limited number of years with positive (wet) values (Fig. 3a, b, and c). For the Czech Republic, Poland, and Spain the driest years have been recorded through the 21st century, while in the case of Norway the driest years have been recorded at the beginning of the 20th century. The strongest drying trend is observed for the Czech Republic (−1.53/139 years), followed by Poland (−1.42/139 years) and Spain (−0.98/ 139 years) (Table 1). In the case of Norway, we observe a significant wetting trend over the analyzed period (1.42/139 years).

The identified hot spots, in terms of drying trend, have been under the influence of a long-lasting drought over the last decade (Ionita et al., 2021; Moravec et al., 2021), with 2015 and 2018 reaching record levels in terms of meteorological and soil moisture drought, especially over the central part of Europe (Ionita et al., 2017; Moravec et al., 2021). The extreme dry summers in 2015 and 2018 have been associated with exceptional cold SST anomalies in the North Atlantic Basin and persistent high-pressure systems over Europe (i.e. atmospheric blocking) (Duchez et al., 2016; Ionita et al., 2017). Overall, on monthly to interannual time-scales, the association between cold central North Atlantic conditions, blocking-like atmospheric circulation patterns, and dry summers in central parts of Europe manifests as a predominant feature of the hydroclimate variability over Europe throughout the observational record (Ionita et al., 2011; Schubert et al., 2014) and also over paleo time-scales (Ionita et al., 2021). On interannual to multidecadal time scales, dry (wet) summers were found to be associated with a cold (warm) North Atlantic basin in the previous winter, reduced (enhanced) winter precipitation over the central part of Europe, and enhanced blocking over the central and northern parts of Europe (Ionita et al., 2021, 2012; Kingston et al., 2012; Schubert et al., 2016). Similarly, it was shown that during the negative phase of AMO (cold North Atlantic basin) Germany and the southern part of the Scandinavian Peninsula is affected by dryness, while a warm North Atlantic basin (positive AMO phase) is associated with wetness over these regions (Ionita et al., 2012).

To investigate the potential drivers of the drying trend over the central and southern part of Europe, we applied the CCA methodology between December SPEI12 and the annual North Atlantic SST over the 1902 – 2020 period (Fig. 4). The main aim of the CCA is to identify coupled modes of variability and their associated temporal components in the SPEI12/ SST data sets. Fig. 4a shows the SST pattern of the first coupled mode (further referred as CCA1-SST), which explains 14.37 % of the total variance. It is dominated by an area of negative SST anomalies south of Greenland surrounded by positive SST anomalies located around the eastern U.S coast and the western European coast and the North Sea. The structure of the CCA1-SST pattern (Fig. 4a) was found to be part of an SST mode
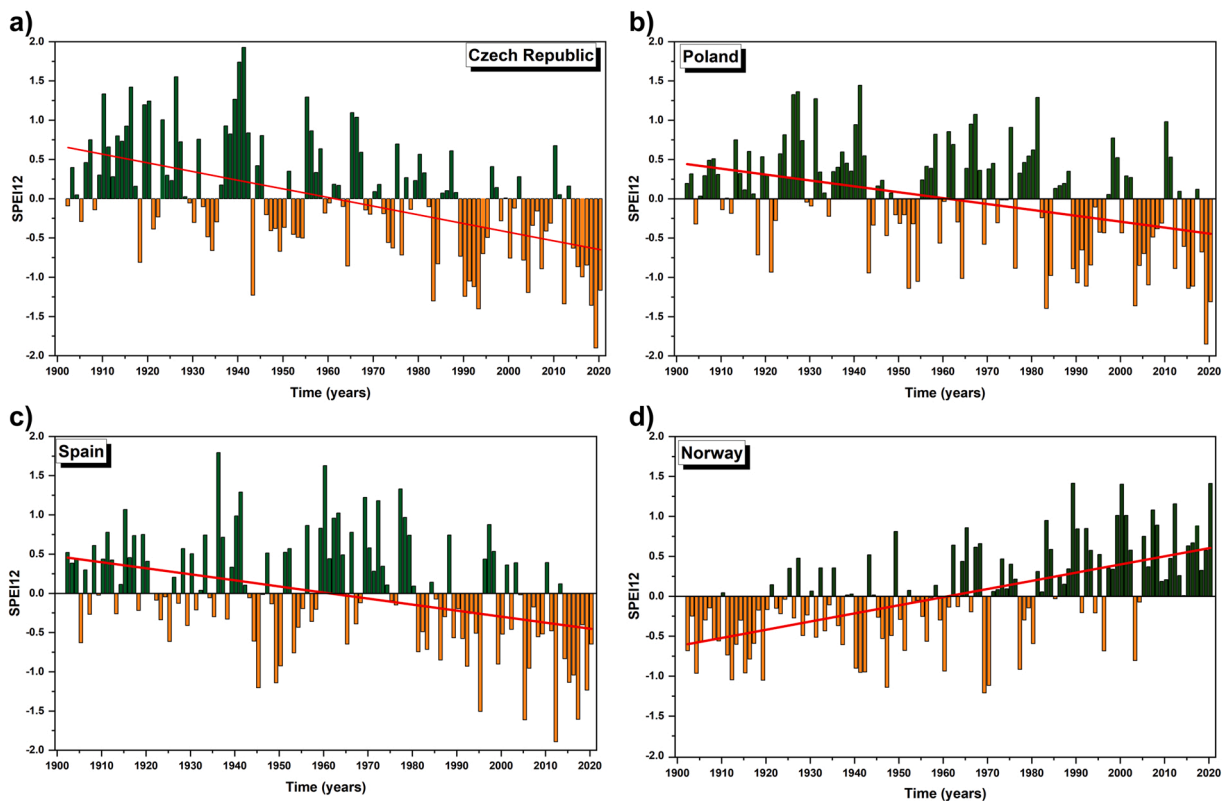

Fig. 3. Temporal evolution of December SPEEI12 averaged over different countries and the associated linear trend (red line): a) the Czech Republic, b) Poland, c) Spain and d) Norway. Green indicates wet years and orange indicates dry years. Analyzed period: 1902–2020.

Table 1

Results of the trend analysis for the December SPEI12 (Figure3) averaged at country level. The trend analysis was conducted based on nonparametric Mann-Kendall test. The analysis was performed over the period 1902 – 2020.

		SPI Trend	P-value
Czech Republic	December SPEI12	-1.53 z-scores/analyzed period	4.02E-09[a]
Poland	December SPEI12	-1.42 z-scores/analyzed period	1.91E-05[a]
Spain	December SPEI12	-0.98 z-scores /analyzed period	2.79E-05[a]
Norway	December SPEI12	1.42 z-scores/ analyzed period	4.79E-09[a]

The null hypothesis of no trend is rejected if the p-values is lower than 0.05 (significance level of α = 0.05).

[a] Indicates a statistically significant trend the 95 % confidence level using the Mann–Kendall test.
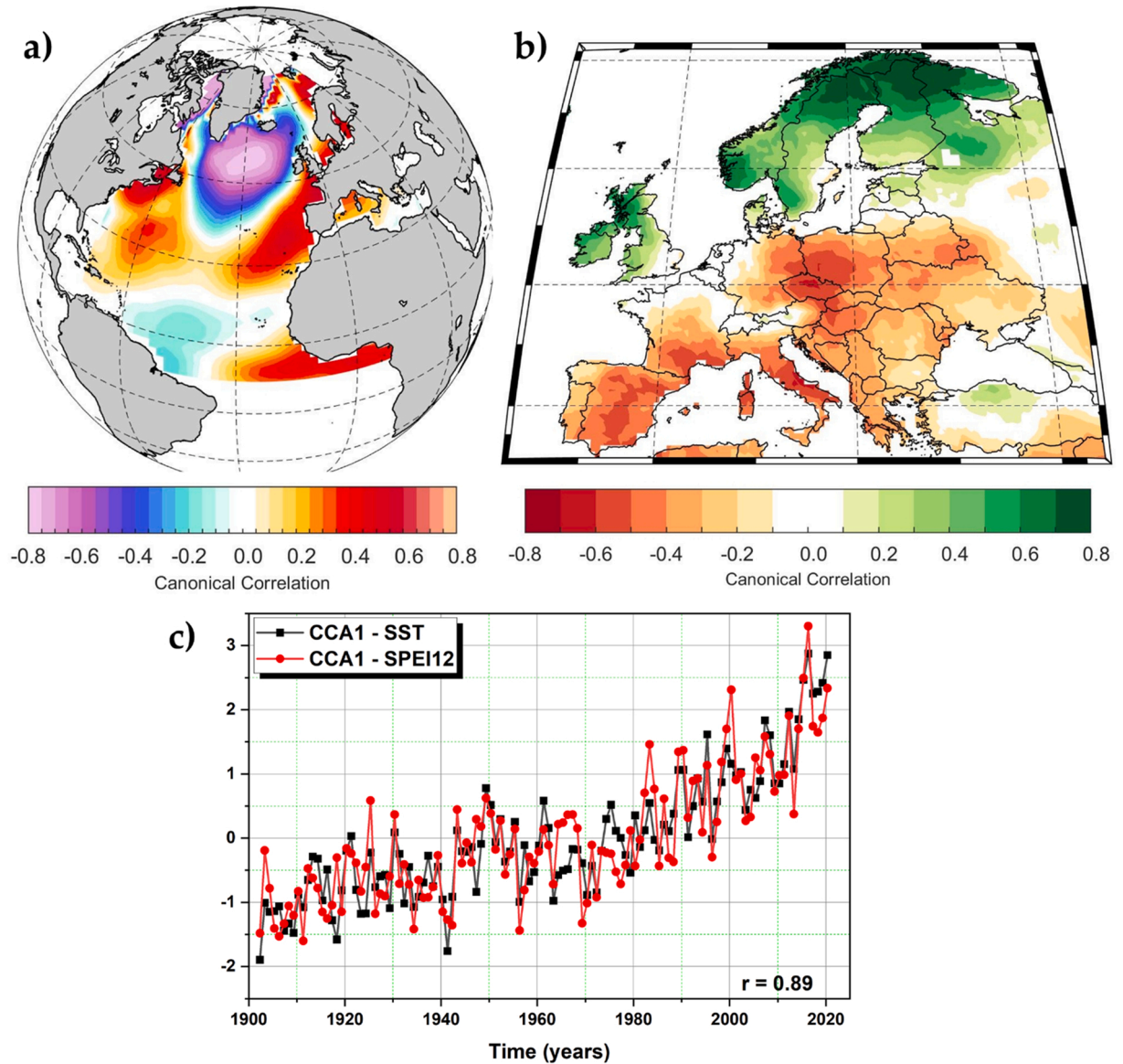

Fig. 4. The first coupled mode of variability between (a) Annual Sea Surface Temperature (SST) and b) December SPEI12 over the period 1902–2020; c) The standardized amplitudes corresponding to CCA1–SST (black line) and CCA1–SPEI12 (red line).

associated with the long-term AMOC weakening trend (Caesar et al., 2018; Dima and Lohmann, 2010), which was attributed to increasing atmospheric CO_2 concentration (Dima et al., 2021). Later on, based on observation data and simulations performed with an oceanic general circulation model, it was shown that this pattern is generated by centennial scale AMOC changes induced by deep water formation changes in the Nordic Seas (Dima et al., 2022; e.g. Fig. 4 and S4 in their study). In particular, the center of negative anomalies located south of Greenland appears to be linked with a weakening of an AMOC cell centered at 50°N. A downslope of deep western boundary current (DWBC), which is fed by the Nordic Seas overflow system, could result in the bottom vortex stretching with corresponding ocean surface changes on the Northern Recirculation Gyre, associated with adjustment of the Gulf Stream position (Born et al., 2009; Langehaug et al., 2012; Yeager and Danabasoglu, 2014; Zhang et al., 2011; Zhang and Vallis, 2006). An anomalous DWBC affects also the subpolar AMOC cell, through geostrophic balance. These processes are consistent with the North Atlantic SST structure (Fig. 4a). One notes that the AMOC trend mode, characterized by centennial-scale changes, is distinct from the multidecadal fluctuations of the overturning circulation (Dima and Lohmann, 2010), which are reflected on the North Atlantic SST as a monopolar pattern and which are associated with the Atlantic Multidecadal Oscillation (AMO; Schlesinger and Ramankutty, 1994). This implies that the atmospheric and SPEI12 changes emphasized here are linked only to centennial-scale variations of AMOC, which are emphasized in climate projections for this century but are not directly reflecting the multidecadal fluctuations of the overturning associated with AMO.

The corresponding December SPEI12 (CCA1-SPEI12) spatial pattern (Fig. 4b), which explains 13.88 % of the total variance, is characterized by a dipole-like structure between the southern and central parts of Europe (negative loadings) and the Scandinavian
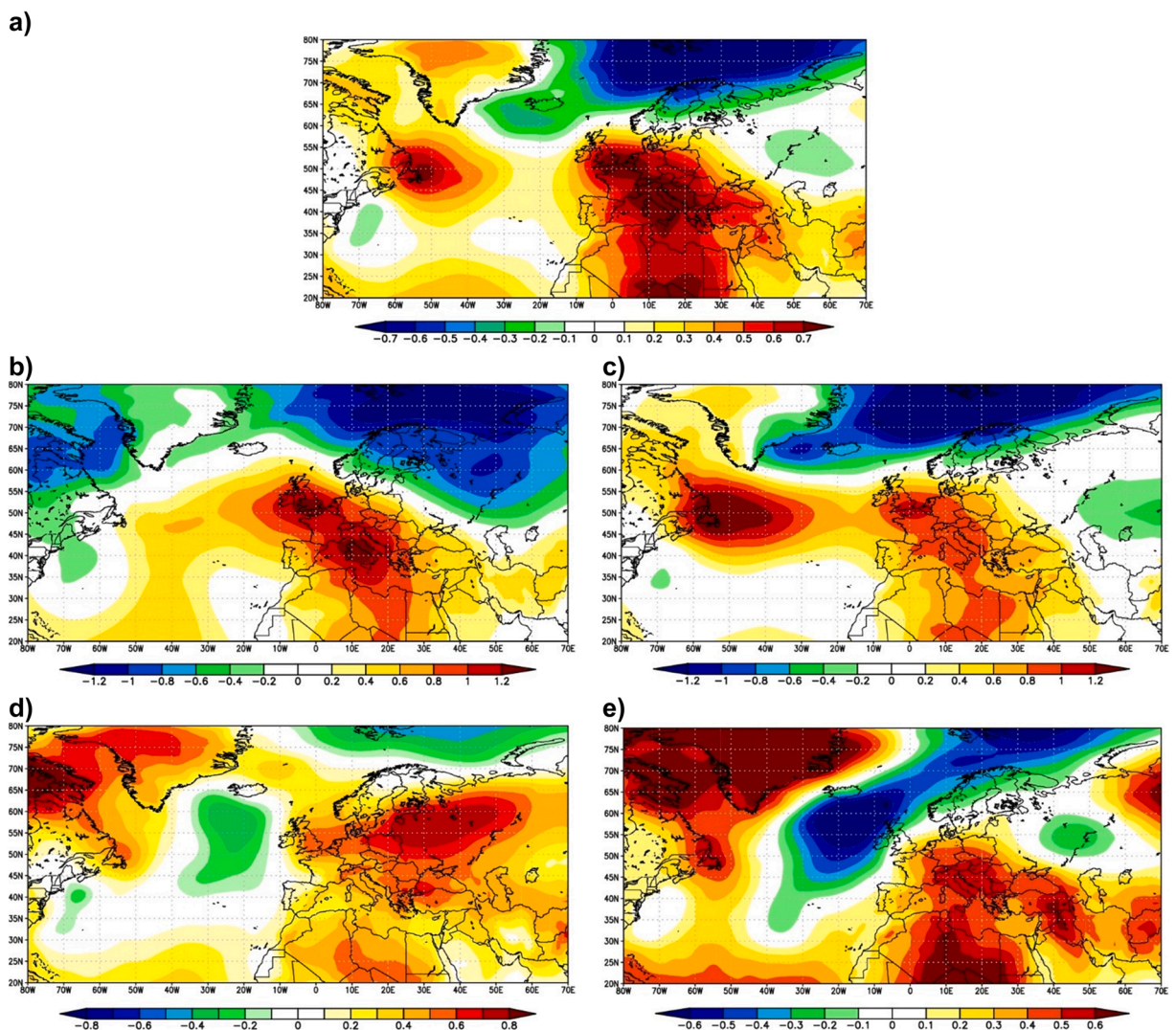

Fig. 5. a) Regression map of the time series corresponding to CCA-SPEI12 on the annual Sea Level Pressure (SLP) field; b) as in a) but for winter (January-February-March) SLP field; c) as in a) but for spring (April-May-June) SLP filed; d) as in a) but for summer (July-August-September) SLP field; and e) as in a) but for autumn (October-November-December) SLP field.

Peninsula and U.K. (positive loadings). The highest negative loadings correspond to the regions/countries where a significant drying trend is observed (i.e., Spain, Portugal, the southern part of France, Italy, the eastern part of Germany, the Czech Republic, Poland, Hungary, Slovenia, and Croatia, see also Fig. 1). Overall, the first CCA pair, which is the focus of our study, and which reflects the coupling between December SPEI12 and the annual SST, indicates that dry (wet) conditions over the southern and central (northern) parts of Europe are associated with negative SST anomalies south of Greenland, flanked by positive SST anomalies over the eastern U.S coast, western European Coast, the North Sea, and the Mediterranean Sea. The dipole-like structure of the CCA1-SPEI12 is a prominent feature of the drought variability at the European scale (Ionita et al., 2015).

This is consistent with the corresponding time-series of the CCA1-SPEI12 and CCA1-SST, which are significantly correlated (r = 0.89, 99 % significance level) and shows a significant centennial trend (e.g., drying over the southern and central parts of Europe is associated with cooling of the North Atlantic basin south of Greenland) over the analyzed period (Fig. 4c). The fact that the North Atlantic cooling was associated with an AMOC weakening (Dima and Lohmann, 2010; Caesar et al., 2018; Dima et al., 2022) implies that the CCA1-SPEI12 pattern could be considered a consequence of Atlantic ocean circulation slowdown.

In order to investigate the mechanisms through which an AMOC weakening and associated negative SST anomalies south of Greenland influence the SPEI12 field, we constructed regression maps of the sea level pressure field on the CCA1 - SPEI12 time components (Fig. 5). The regression of the annual SLP field on the time series of CCA1 – SPEI12 (Fig. 5a), indicates that dry conditions over the southern and central parts of Europe are associated with a high-pressure system extending from the east coast of the U.S. to the central and southern parts of Europe (where it reaches the highest amplitude) and a low-pressure system over Fennoscandia and the Arctic region. The mechanisms linking the CCA1 - SPEI12 pattern with this atmospheric structure are revealed also by the corresponding regression maps constructed between the seasonal SLP field (i.e., January – February – March (Fig. 5b), April – May - June (Fig. 5c), July – August – September (Fig. 5d) and October – November – December (Fig. 5e)) and the time series of CCA1 – SPEI12. The winter SLP regression map resembles the positive phase of the North Atlantic Oscillation (NAO) (Fig. 5b) and is consistent with a
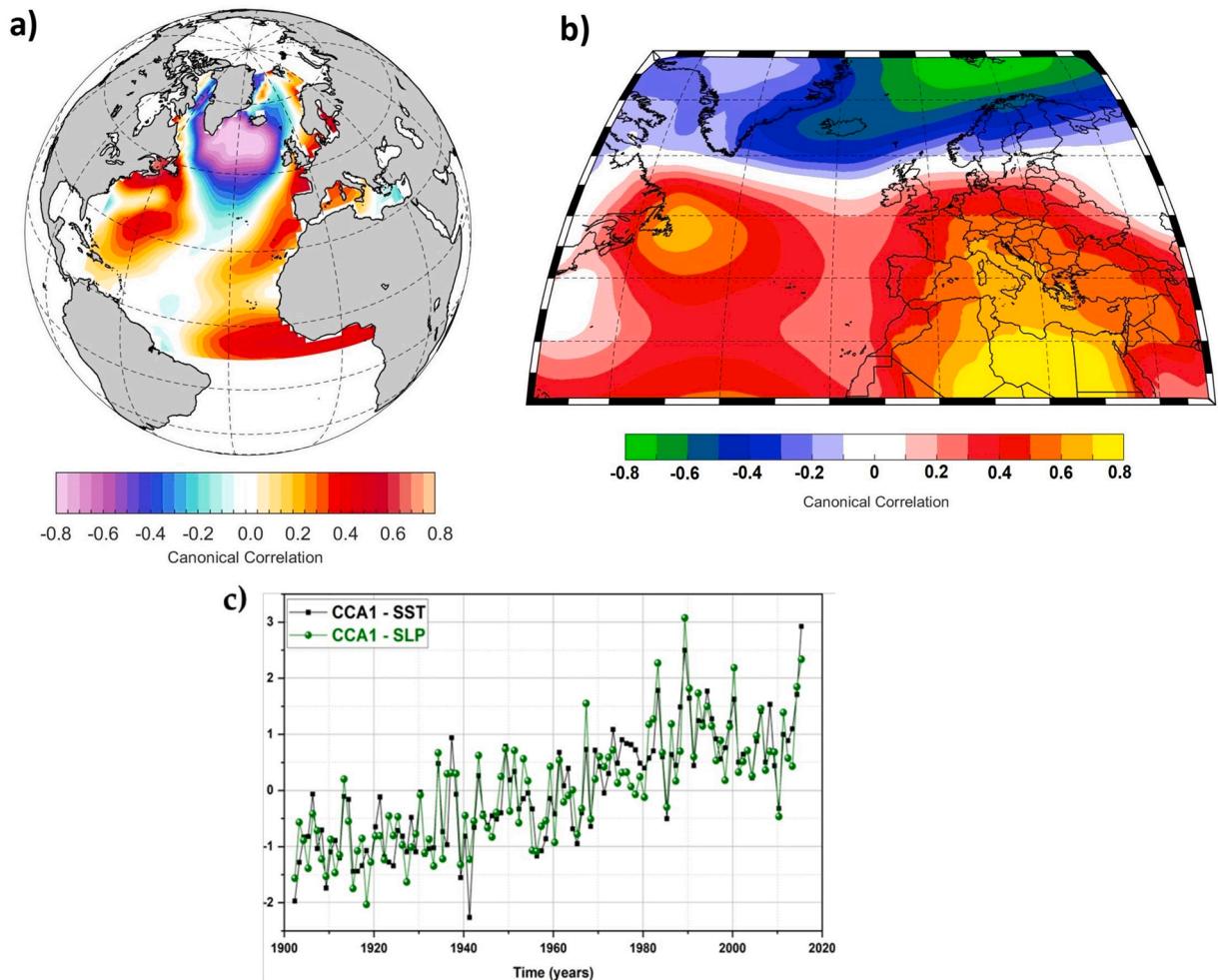

Fig. 6. The first coupled mode of variability between (a) Annual Sea Surface Temperature (SST) and b) Annual SLP over the period 1902–2020; c) The standardized amplitudes corresponding to CCA1–SST (black line) and CCA1–SLP (green line). Explained variance: SST (12 %) and SLP (19 %).

barotropic atmospheric response to the north-south SST gradient disposed south of Greenland, in the CCA1-SST pattern (Rodwell et al., 1999) (Fig. 4b). Our findings are also in agreement with the study of (Rousi et al., 2021) which has shown that an AMOC decline leads to ~60 % increase in an anticyclonic (i.e. high pressure) circulation over the western and central parts of Europe, with a significant effect on the central European droughts.

The high-pressure system over the central and southern parts of Europe suppresses ascending motions, and reduces water vapor condensation and precipitation formation, leading to drought conditions below this system. This high-pressure system over the central and southern parts of Europe has a seasonally persistent feature (Fig. 5b-e), thus leading to long-lasting droughts by suppressing precipitation and/or increasing the temperature. Thus, based on these results, we argue that the long-term drying trend observed over the southern and central parts of Europe is driven by an association between a relatively high frequency of atmospheric blocking conditions (e.g., persistent high-pressure systems) induced by the centennial scale trend of SSTs disposed south of Greenland. This specific SST pattern was associated with a long term weakening trend of the AMOC, in response to increasing atmospheric CO_2 concentrations (Caesar et al., 2018; Dima et al., 2021).

The influence of the prolonged positive SLP anomalies on the drying trend over the central part of Europe is supported also by the first coupled mode of variability between the annual SST and the annual SLP filed. The spatial structure of the first coupled mode of variability SST/SLP (Fig. 6) is similar to the SST pattern associated with the drying trend over central Europe (Fig. 3a) and the annual SLP regression map (Fig. 5a). Thus, we can argue that the coupling between the AMOC trend mode and prolonged positive SLP anomalies over the central north Atlantic Basin extending up to central Europe are leading to drying especially in the central and southern parts of Europe.

The influence of AMOC on the North Atlantic large-scale atmospheric circulation is made mainly through the SST anomalies it generates in this sector. Consequently, the structure and mechanism of atmospheric response depend on the corresponding thermal structure of the ocean surface. Two distinct SST patterns were emphasized in associations with AMOC changes (Park and Latif 2008; Dima and Lohmann, 2010; Dima et al., 2022). On one side, multidecadal AMOC variations associated with AMO are associated with a monopolar North Atlantic SST pattern which induces a thermal baroclinic atmospheric response, which projects onto NAO (Sutton and Hodson, 2007). The corresponding axis of the SLP dipole is not zonally aligned, but it is tilted north-eastward (Dima and Lohmann, 2007). On the other side, centennial-scale AMOC changes are reflected by the SST dipole located south of Greenland. This patterns increases the local meridional temperature gradient, which in turn favors the formation of storms which can feed with energy the zonal circulation and result in a NAO-like barotropic atmospheric response (Frankignoul et al., 2013; Rodwell et al., 1999). This type of atmospheric response (i.e., NAO like barotropic), which has an impact on the European climate, can be observed in Figs. 5 and 6 and resembles the barotropic atmospheric response to the AMOC centennial scale changes, reflected by the SST dipole located south of Greenland. One notes that at both time scales, an AMOC weakening induces a positive NAO-like response in the atmosphere.

The causal relationship between the North Atlantic SST pattern and the corresponding SPEI12 structure derived through CCA has been also tested by using the CCM method, which was applied to the corresponding two time-series (Fig. 4c). The cross-map skill from the time component of the SPEI12 and the time component to the North Atlantic SST identified through CCA increases with the library length and reaches a plateau around $\rho \approx 0.85$, well above the 95 % significance level, indicating a robust causal relationship from the later to the former (Fig. 7).

4. Discussion and conclusions

In this study, we have investigated the spatio-temporal variability of the annual drought variability over Europe, as represented by SPEI12, and related the long-term drying trend over the central and southern parts of Europe with large-scale atmospheric and oceanic anomalies. The relationship between December SPEI12, which reflects an integration of moisture availability through the whole year,
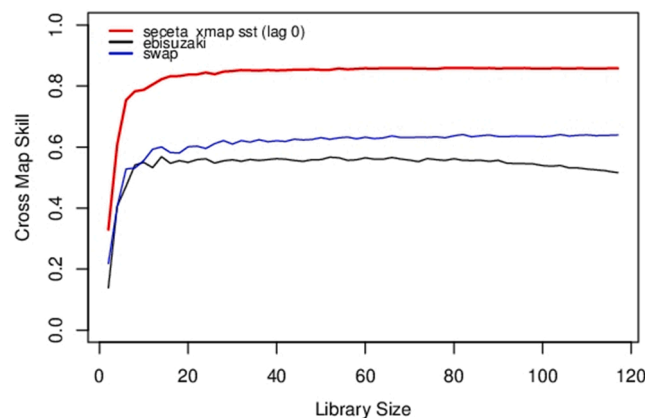

Fig. 7. Cross map skill (red line) given by the correlation between predicted and observed values, as a function of library length for the SST and SPEI12 time components. The blue (black) lines correspond to the 95th cross map between each affected variable and the surrogate of the cause generated by a swap (Ebisuzaki) model. The variables have the embedding dimension, E = 8 and embedding lag = 0.

and annual SST was analyzed by using canonical correlation analysis and Convergent Cross-Mapping methods. We have focused the current study just on the first mode of coupled variability since we aimed to identify the drivers of the drying/wetting trend patterns at European scale. The coupled modes of variability, as identified by the CCA, can provide insights into the teleconnection patterns between the long-term drought conditions over Europe and global/regional SST patterns. These indicate that the long-term drying trend in the southern and central parts of Europe, as captured by SPEI12, is linked with a dipolar SLP pattern, which resembles the positive phase of NAO, but with the Azore center shifted towards Europe, which is reminiscent of a barotropic response to a SST structure located south of Greenland, in response to the long-term weakening trend of the AMOC.

The relationship between a weak AMOC state and long-lasting drought over Europe seems to be a pervasive one through different time scales and climate backgrounds. In a recent study (Ionita et al., 2021), have found that long-lasting droughts over the central part of Europe, over the last millennium, have been driven by a combination of low solar variability, a weak AMOC state characterized by negative SST anomalies south of Greenland, and high atmospheric blocking frequency over the central part of Europe. From an even longer time span perspective, the 8.2ka BP climatic event, which occurred during a period of a relatively warm climate background, and was likely associated with a significant reduction of the AMOC intensity (von Grafenstein et al., 1998), and can be seen as an analog for the current and future oceanic and hydro-climatic configuration. Consistent with our results, an abrupt surface cooling of the North Atlantic basin, which indicated a weakening of AMOC, at ~8.2ka lead to enhanced drying over the western part of Europe. Further back in time, for the Younger Dryas fluctuation (about 12,900–11,700 years BP), a strong cooling of the North Atlantic Ocean in response to a reduction of the AMOC, corroborated with enhanced blocking activity, has been associated with harsh winters and warm summers over Europe (Schenk et al., 2018). Therefore, the connections between the North Atlantic Ocean and dryness/wetness over Europe appear to represent a pervasive manifestation through climatic events manifested in both, recent and distant past.

Future climate projections indicate that Europe will face substantial drying, even for the less aggressive pathways scenarios (SSP126 and SSP245) (Balting et al., 2021). As climate projections show a long-term slowdown of AMOC during this century (Collins et al., 2013), our results imply additional drought risk, next to the one driven by the global warming signal, in the central and southern parts of Europe in the upcoming decades.

Data availability

The data that support the findings of this study are available from the corresponding author upon reasonable request.

CRediT authorship contribution statement

Monica Ionita: Conceptualization, Methodology, Writing – original draft, **Mihai Dima:** Conceptualization, Methodology, Writing – original draft, **Viorica Nagavciuc:** Conceptualization, Methodology, **Patrick Scholz:** Methodology and software.

Declaration of Competing Interest

The authors declare the following financial interests/personal relationships which may be considered as potential competing interests: Monica Ionita reports financial support and article publishing charges were provided by Alfred Wegener Institute for Polar and Marine Research. Viorica Nagavciuc reports financial support was provided by Executive Unit for Financing Higher Education Research Development and Innovation.

Data availability

The authors do not have permission to share data.

Appendix A. Supporting information

Supplementary data associated with this article can be found in the online version at doi:10.1016/j.ejrh.2022.101176.

References

Adamowski, K., Prokoph, A., Adamowski, J., 2009. Development of a new method of wavelet aided trend detection and estimation. Hydrol. Process. 23, 2686–2696. https://doi.org/10.1002/hyp.7260.

Bakke, S.J., Ionita, M., Tallaksen, L.M., 2020. The 2018 northern European hydrological drought and its drivers in a historical perspective. Hydrol. Earth Syst. Sci. 24, 1–44. https://doi.org/10.5194/hess-2020-239.

Balting, D.F., AghaKouchak, A., Lohmann, G., Ionita, M., 2021. Northern Hemisphere drought risk in a warming climate. NPJ Clim. Atmos. Sci. 4, 61. https://doi.org/10.1038/s41612-021-00218-2.

Born, A., Levermann, A., Mignot, J., 2009. Sensitivity of the Atlantic ocean circulation to a hydraulic overflow parameterisation in a coarse resolution model: Response of the subpolar gyre. Ocean Model 27, 130–142. https://doi.org/10.1016/j.ocemod.2008.11.006.

Caesar, L., Rahmstorf, S., Robinson, A., Feulner, G., Saba, V., 2018. Observed fingerprint of a weakening Atlantic Ocean overturning circulation. Nature 556, 191–196. https://doi.org/10.1038/s41586-018-0006-5.

Collins, M., Knutti, R., Arblaster, J., Dufresne, J.-L., Fichefet, T., Friedlingstein, P., Gao, X., Gutowski, W.J., Johns, T., Krinner, G., Shongwe, M., Tebaldi, C., Weaver, A.J., Wehner, M., 2013. Long-term climate change: projections, commitments and irreversibility. In: Stocker, T.F., Qin, D., Plattner, G.-K., Tignor, M., Allen, S.K., Boschung, J., Nauels, A., Xia, Y., Bex, V., Midgley, P.M. (Eds.), Climate Change 2013: The Physical Science Basis. Contribution of Working Group I to the Fifth Assessment Report of the Intergovernmental Panel on Climate Change. Cambridge University Press, Cambridge, United Kingdom and New York, NY, USA, pp. 1029–1136. https://doi.org/10.1017/CBO9781107415324.024.

Cook, E.R., Solomina, O., Matskovsky, V., Cook, B.I., Agafonov, L., Berdnikova, A., Dolgova, E., Karpukhin, A., Knysh, N., Kulakova, M., Kuznetsova, V., Kyncl, T., Kyncl, J., Maximova, O., Panyushkina, I., Seim, A., Tishin, D., Ważny, T., Yermokhin, M., 2020. The European Russia Drought Atlas (1400–2016 CE). Clim. Dyn. 54, 2317–2335. https://doi.org/10.1007/s00382-019-05115-2.

Dang, V.H., Tran, D.D., Cham, D.D., Hang, P.T.T., Nguyen, H.T., Truong, H., Van, Tran, P.H., Duong, M.B., Nguyen, N.T., Le, K., Van, Pham, T.B.T., Nguyen, A.H., 2020. Assessment of rainfall distributions and characteristics in coastal provinces of the Vietnamese Mekong delta under climate change and ENSO processes. Water 12. https://doi.org/10.3390/w12061555.

Dima, M., Lohmann, G., 2007. A Hemispheric mechanism for the atlantic multidecadal oscillation. J. Clim. 20, 2706–2719. https://doi.org/10.1175/JCLI4174.1.

Dima, M., Lohmann, G., 2010. Evidence for two distinct modes of large-scale ocean circulation changes over the last century. J. Clim. 23, 5–16. https://doi.org/10.1175/2009JCLI2867.1.

Dima, M., Nichita, D.R., Lohmann, G., Ionita, M., Voiculescu, M., 2021. Early-onset of Atlantic meridional overturning circulation weakening in response to atmospheric CO_2 concentration. NPJ Clim. Atmos. Sci. 4. https://doi.org/10.1038/s41612-021-00182-x.

Dima, M., Lohmann, G., Ionita, M., Knorr, G., Scholz, P., 2022. AMOC modes linked with distinct North Atlantic deep water formation sites. Clim. Dyn. https://doi.org/10.1007/s00382-022-06156-w.

Duchez, A., Frajka-Williams, E., Josey, S.A., Evans, D.G., Grist, J.P., Marsh, R., McCarthy, G.D., Sinha, B., Berry, D.I., Hirschi, J.J.M., 2016. Drivers of exceptionally cold North Atlantic Ocean temperatures and their link to the 2015 European heat wave. Environ. Res. Lett. 11. https://doi.org/10.1088/1748-9326/11/7/074004.

EEA, 2019. Economic Losses from Climate-related Extremes in Europe. European Environment Agency.

Frankignoul, C., Gastineau, G., Kwon, Y.-O., 2013. The influence of the AMOC variability on the atmosphere in CCSM3. J. Clim. 26, 9774–9790. https://doi.org/10.1175/JCLI-D-12-00862.1.

von Grafenstein, U., Erlenkeuser, H., Müller, J., Jouzel, J., Johnsen, S., 1998. The cold event 8200 years ago documented in oxygen isotope records of precipitation in Europe and Greenland. Clim. Dyn. 14, 73–81. https://doi.org/10.1007/s003820050210.

Hari, V., Rakovec, O., Markonis, Y., Hanel, M., Kumar, R., 2020. Increased future occurrences of the exceptional 2018–2019 Central European drought under global warming. Sci. Rep. 10, 12207. https://doi.org/10.1038/s41598-020-68872-9.

Harris, I., Osborn, T.J., Jones, P., Lister, D., 2020. Version 4 of the CRU TS monthly high-resolution gridded multivariate climate dataset. Sci. Data 7, 1–18. https://doi.org/10.1038/s41597-020-0453-3.

Ionita, M., Nagavciuc, V., 2020. Forecasting low flow conditions months in advance through teleconnection patterns, with a special focus on summer 2018. Sci. Rep. 10, 13258. https://doi.org/10.1038/s41598-020-70060-8.

Ionita, M., Nagavciuc, V., 2021. Changes in drought features at the European level over the last 120 years. Nat. Hazards Earth Syst. Sci. https://doi.org/10.5194/nhess-21-1685-2021.

Ionita, M., Rimbu, N., Lohmann, G., 2011. Decadal variability of the Elbe River streamflow. Int. J. Clim. 31. https://doi.org/10.1002/joc.2054.

Ionita, M., Lohmann, G., Rimbu, N., Chelcea, S., Dima, M., 2012. Interannual to decadal summer drought variability over Europe and its relationship to global sea surface temperature. Clim. Dyn. 38, 363–377. https://doi.org/10.1007/s00382-011-1028-y.

Ionita, M., Boroneanț, C., Chelcea, S., 2015. Seasonal modes of dryness and wetness variability over Europe and their connections with large scale atmospheric circulation and global sea surface temperature. Clim. Dyn. 45, 2803–2829. https://doi.org/10.1007/s00382-015-2508-2.

Ionita, M., Tallaksen, L.M., Kingston, D.G., Stagge, J.H., Laaha, G., Lanen, H.A.J., Van, Scholz, P., Chelcea, S.M., Haslinger, K., Van Lanen, H.A.J., Scholz, P., Chelcea, S.M., Haslinger, K., Lanen, H.A.J., Van, Chelcea, S.M., Haslinger, K., Scholz, P., Chelcea, S.M., Haslinger, K., 2017. The European 2015 drought from a climatological perspective. Hydrol. Earth Syst. Sci. 21, 1397–1419. https://doi.org/10.5194/hess-21-1397-2017.

Ionita, M., Nagavciuc, V., Guan, B., 2020. Rivers in the sky, flooding on the ground: the role of atmospheric rivers in inland flooding in central Europe. Hydrol. Earth Syst. Sci. 24, 5125–5147. https://doi.org/10.5194/hess-24-5125-2020.

Ionita, M., Dima, M., Nagavciuc, V., Scholz, P., Lohmann, G., 2021. Past megadroughts in central Europe were longer, more severe and less warm than modern droughts. Commun. Earth Environ. 2, 61. https://doi.org/10.1038/s43247-021-00130-w.

IPCC, 2018. Global warming of 1.5°C An An IPCC Special Report on the impacts of global warming of 1.5°C above pre-industrial levels and related global greenhouse gas emission pathways, in the context of strengthening the global response to the threat of climate chang. Geneva, Switzerland. ⟨https://doi.org/10.1017/CBO9781107415324⟩.

Jackson, L.C., Wood, R.A., 2020. Fingerprints for early detection of changes in the AMOC. J. Clim. 33, 7027–7044. https://doi.org/10.1175/JCLI-D-20-0034.1.

Kingston, D.G., Fleig, A.K., Tallaksen, L.M., Hannah, D.M., 2012. Ocean-atmosphere forcing of summer streamflow drought in Great Britain, 121026084711009 J. Hydrometeorol.. https://doi.org/10.1175/JHM-D-11-0100.1.

Kingston, D.G., Stagge, J.H., Tallaksen, L.M., Hannah, D.M., 2015. European-scale drought: understanding connections between atmospheric circulation and meteorological drought indices. J. Clim. 28, 505–516. https://doi.org/10.1175/JCLI-D-14-00001.1.

Langehaug, H.R., Medhaug, I., Eldevik, T., Otterå, O.H., 2012. Arctic/Atlantic exchanges via the subpolar gyre. J. Clim. 25, 2421–2439. https://doi.org/10.1175/JCLI-D-11-00085.1.

Liu, W., Xie, S.-P., Liu, Z., Zhu, J., 2017. Overlooked possibility of a collapsed Atlantic Meridional Overturning Circulation in warming climate. Sci. Adv. 3, 1–8. https://doi.org/10.1126/sciadv.1601666.

Liu, W., Fedorov, A.V., Xie, S.P., Hu, S., 2020. Climate impacts of a weakened Atlantic meridional overturning circulation in a warming climate. Sci. Adv. 6, 1–9. https://doi.org/10.1126/sciadv.aaz4876.

Mann, H.B., 1945. Non-parametric test against trend. Econometrica 13, 245–259. https://doi.org/10.2307/1907187.

Moravec, V., Markonis, Y., Rakovec, O., Svoboda, M., Trnka, M., Kumar, R., Hanel, M., 2021. Europe under multi-year droughts: how severe was the 2014–2018 drought period. Environ. Res. Lett. 16. https://doi.org/10.1088/1748-9326/abe828.

Naumann, G., Alfieri, L., Wyser, K., Mentaschi, L., Betts, R.A., Carrao, H., Spinoni, J., Vogt, J., Feyen, L., 2018. Global changes in drought conditions under different levels of warming. Geophys. Res. Lett. 45, 3285–3296. https://doi.org/10.1002/2017GL076521.

Naumann, G., Cammalleri, C., Mentaschi, L., Feyen, L., 2021. Increased economic drought impacts in Europe with anthropogenic warming. Nat. Clim. Chang. 11, 485–491. https://doi.org/10.1038/s41558-021-01044-3.

Park, W., Latif, M., 2008. Multidecadal and multicentennial variability of the meridionaloverturning circulation. Geophys. Res. Lett. 35 (22), L22703 https://doi.org/10.1029/2008GL035779.

Rahmstorf, S., Box, J.E., Feulner, G., Mann, M.E., Robinson, A., Rutherford, S., Schaffernicht, E.J., Schaaernicht, E.J., 2015. Exceptional twentieth-century slowdown in Atlantic Ocean overturning circulation. Nat. Clim. Chang. 5, 475–480. https://doi.org/10.1038/NCLIMATE2554.

Rayner, N.A., Parker, D.E.E., Horton, E.B.B., Folland, C.K., Alexander, L.V.V., Rowell, D.P.P., Kent, E.C., Kaplan, A., 2003. Global analyses of sea surface temperature, sea ice, and night marine air temperature since the late nineteenth century. J. Geophys. Res. Atmos. 108, 4407. https://doi.org/10.1029/2002JD002670.

Rodwell, M.J., Rowell, D.P., Folland, C.K., 1999. Oceanic forcing of the wintertime North Atlantic Oscillation and European climate. Nature 398, 320–323. https://doi.org/10.1038/18648.

Rousi, E., Selten, F., Rahmstorf, S., Coumou, D., 2021. Changes in North Atlantic atmospheric circulation in a warmer climate favor winter flooding and summer drought over Europe. J. Clim. 34, 2277–2295. https://doi.org/10.1175/JCLI-D-20-0311.1.

Schenk, F., Väliranta, M., Muschitiello, F., Tarasov, L., Heikkilä, M., Björck, S., Brandefelt, J., Johansson, A.V., Näslund, J.O., Wohlfarth, B., 2018. Warm summers during the Younger Dryas cold reversal. Nat. Commun. 9. https://doi.org/10.1038/s41467-018-04071-5.

Schlesinger, M.E., Ramankutty, N., 1994. An oscillation in the global climate system of period 65-70 years. Nature 367, 723–726.

Schubert, S.D., Wang, H., Koster, R.D., Suarez, M.J., Groisman, P.Y., 2014. Northern Eurasian heat waves and droughts. J. Clim. 27, 3169–3207. https://doi.org/10.1175/JCLI-D-13-00360.1.

Schubert, S.D., Stewart, R.E., Wang, H., Barlow, M., Berbery, E.H., Cai, W., Hoerling, M.P., Kanikicharla, K.K., Koster, R.D., Lyon, B., Mariotti, A., Mechoso, C.R., Müller, O.V., Rodriguez-Fonseca, B., Seager, R., Senevirante, S.I., Zhang, L., Zhou, T., 2016. Global meteorological drought: a synthesis of current understanding with a focus on sst drivers of precipitation deficits. J. Clim. https://doi.org/10.1175/JCLI-D-15-0452.1.

Schuldt, B., Buras, A., Arend, M., Vitasse, Y., Beierkuhnlein, C., Damm, A., Gharun, M., Grams, T.E.E., Hauck, M., Hajek, P., Hartmann, H., Hiltbrunner, E., Hoch, G., Holloway-Phillips, M., Körner, C., Larysch, E., Lübbe, T., Nelson, D.B., Rammig, A., Rigling, A., Rose, L., Ruehr, N.K., Schumann, K., Weiser, F., Werner, C., Wohlgemuth, T., Zang, C.S., Kahmen, A., 2020. A first assessment of the impact of the extreme 2018 summer drought on Central European forests. Basic Appl. Ecol. 45, 86–103. https://doi.org/10.1016/j.baae.2020.04.003.

Sen, P.K., 1968. Estimates of the regression coefficient based on Kendall's Tau. J. Am. Stat. Assoc. 63, 1379–1389. https://doi.org/10.1080/01621459.1968.10480934.

Slivinski, L.C., Compo, G.P., Sardeshmukh, P.D., Whitaker, J.S., McColl, C., Allan, R.J., Brohan, P., Yin, X., Smith, C.A., Spencer, L.J., Vose, R.S., Rohrer, M., Conroy, R.P., Schuster, D.C., Kennedy, J.J., Ashcroft, L., Brönnimann, S., Brunet, M., Camuffo, D., Cornes, R., Cram, T.A., Domínguez-Castro, F., Freeman, J.E., Gergis, J., Hawkins, E., Jones, P.D., Kubota, H., Lee, T.C., Lorrey, A.M., Luterbacher, J., Mock, C.J., Przybylak, R.K., Pudmenzky, C., Slonosky, V.C., Tinz, B., Trewin, B., Wang, X.L., Wilkinson, C., Wood, K., Wyszynski, P., 2021. An evaluation of the performance of the twentieth century reanalysis version 3. J. Clim. 34, 1417–1438. https://doi.org/10.1175/JCLI-D-20-0505.1.

Spinoni, J., Nuamann, G., Vogt, J.V., Barbosa, P., Naumann, G., Vogt, J.V., Barbosa, P., 2016. Meteorological droughts in Europe: events and impacts - past trends and future projections. Luxemb., EUR 27748 EN, EUR 27748 EN. https://doi.org/10.2788/79637.

Spinoni, J., Vogt, J.V., Barbosa, P., Dosio, A., McCormick, N., Bigano, A., Füssel, H.M., 2018. Changes of heating and cooling degree-days in Europe from 1981 to 2100. Int. J. Climatol. 38, e191–e208. https://doi.org/10.1002/joc.5362.

Spinoni, J., Barbosa, P., De Jager, A., McCormick, N., Naumann, G., Vogt, J.V., Magni, D., Masante, D., Mazzeschi, M., 2019. A new global database of meteorological drought events from 1951 to 2016. J. Hydrol. Reg. Stud. 22, 100593 https://doi.org/10.1016/j.ejrh.2019.100593.

Stahl, K., Kohn, I., Blauhut, V., Urquijo, J., De Stefano, L., Acácio, V., Dias, S., Stagge, J.H., Tallaksen, L.M., Kampragou, E., Van Loon, A.F., Barker, L.J., Melsen, L.A., Bifulco, C., Musolino, D., de Carli, A., Massarutto, A., Assimacopoulos, D., Van Lanen, H.A.J.J., 2016. Impacts of European drought events: insights from \hack {\newline} an international database of text-based reports. Nat. Hazards Earth Syst. Sci. 16, 801–819. https://doi.org/10.5194/nhess-16-801-2016.

von Storch, H., Zwiers, F.W., 1999. Statistical Analysis in Climate Research, Statistical Analysis in Climate Research. Cambridge University Press. https://doi.org/10.1017/cbo9780511612336.

Sugihara, G., May, R., Ye, H., Hsieh, C.H., Deyle, E., Fogarty, M., Munch, S., 2012. Detecting causality in complex ecosystems. Science 338 (80), 496–500. https://doi.org/10.1126/science.1227079.

Sutton, R.T., Hodson, D.L.R., 2007. Climate response to basin-scale warming and cooling of the North Atlantic Ocean. J. Clim. 20, 891–907.

Vanderlinden, K., Giráldez, J.V., Meirvenne, M.Van, 2008. Spatial estimation of reference evapotranspiration in Andalusia, Spain. J. Hydrometeorol. 9, 242–255. https://doi.org/10.1175/2007JHM880.1.

Vellinga, M., Wood, R.A., 2008. Impacts of thermohaline circulation shutdown in the twenty-first century. Clim. Change 91, 43–63. https://doi.org/10.1007/s10584-006-9146-y.

Vicente-Serrano, S.M.M., Beguería, S., López-Moreno, J.I.I., 2010. A multiscalar drought index sensitive to global warming: The standardized precipitation evapotranspiration index. J. Clim. 23, 1696–1718. https://doi.org/10.1175/2009JCLI2909.1.

Yeager, S., Danabasoglu, G., 2014. The origins of late-twentieth-century variations in the large-scale North Atlantic circulation. J. Clim. 27, 3222–3247. https://doi.org/10.1175/JCLI-D-13-00125.1.

Zhang, R., Vallis, G.K., 2006. Impact of great salinity anomalies on the low-frequency variability of the North Atlantic climate. J. Clim. 19, 470–482. https://doi.org/10.1175/JCLI3623.1.

Zhang, R., Delworth, T.L., Rosati, A., Anderson, W.G., Dixon, K.W., Lee, H.C., Zeng, F., 2011. Sensitivity of the North Atlantic Ocean Circulation to an abrupt change in the Nordic Sea overflow in a high resolution global coupled climate model. J. Geophys. Res. Ocean. 116, 1–14. https://doi.org/10.1029/2011JC007240.